

Design of a Novel UWB Microstrip Antenna with SIW Feed

Abbas Ebrahimi and Hamid Khodabakhshi*

Abstract—Antenna miniaturization, which is a requirement of modern wireless communication systems, is usually concomitant with the reduction of impedance bandwidth. On the other hand, small antennas should also possess stable radiation patterns across a broad frequency band, such as in UWB systems. In this paper, we propose a UWB antenna structure with a novel feeding system composed of an open cavity resonator. It has a wide relative bandwidth (of about 120%) particularly at the lower frequency limits. The variation of radiation pattern across its operating bandwidth is also negligible. The proposed antenna with the novel feed system is smaller and has a wider frequency bandwidth than other available UWB antennas in the literature. Furthermore, another antenna is proposed, which has a feeding system composed of a surface integrated resonator cavity, fabricated on a two-layer microstrip structure. It has achieved better miniaturization and bandwidth, albeit somewhat lower gain. Three prototype models of the proposed antennas are fabricated and measured, of which the frequency response is in excellent agreement with computer simulation results.

1. INTRODUCTION

Ultra-wideband (UWB) communication systems in the allocated band 3.1 to 10.6 GHz find extensive commercial and military applications. They possess various advantages, such as low power consumption (a necessary condition for wireless communication systems and reduction of adverse effects on the human body), high security (required for secure communication and military systems), immunity to adverse interference (required for the maintenance of some signal level in a limited frequency band under the condition of severe noise in most parts of the band), desirable performance in multipath channels and capability of high signal penetration [1, 2].

Broadband and frequency-independent antennas, such as log-periodic antennas, Vivaldi antennas and TEM horns are not appropriate for UWB communication systems since they suffer from frequency-dependent phase center [1–4]. The printed UWB antenna is preferred because of small size, low profile and low cost. Because of their structure, the phase center is not important for the printed UWB antennas [18].

Microstrip antennas are inherently narrow band. There are several techniques to enhance their bandwidths, such as increase of substrate height [5], low substrate dielectric constant [3], application of special feeding systems [5], implementation of impedance matching techniques [6], use of parasitic elements [7], employment of fractal geometries [5] and application of slot antenna configurations [4, 7]. Furthermore, monopole, coplanar and slot structures have been used for UWB designs, which have lower radiation efficiency than microstrip patch antennas [8].

The length of a square patch is usually equal to $(\lambda/2\sqrt{\epsilon_r})$, where λ is the wavelength in free space, and ϵ_r is the dielectric constant of substrate. Various techniques have been employed for the antenna miniaturization [8], but they all have fundamental limitations, such as the decrease of impedance

Received 27 October 2017, Accepted 23 January 2018, Scheduled 2 February 2018

* Corresponding author: Hamid Khodabakhshi (khodabakhshi.hamid@gmail.com).

The authors are with the Department of Telecommunication, College of Electrical Engineering, Yadegar-E-Imam Khomeini (RAH) Share Rey Branch, Islamic Azad University, Tehran, Iran.

bandwidth due to the reduction of antenna size. In other words, the antenna size and impedance bandwidth are more or less proportional, but they have a complicated relationship.

The implementation of substrate integrated waveguides (SIW) on printed circuit boards (PCB) has been used in the microwave and millimeter wave integrated circuits, such as filters, couplers, dividers, slot antenna arrays, circulators and multiport circuits [10]. The SIW configuration is shown in Fig. 1, where the following relationships should hold [11–13], which are required to remove any gap in the design frequency band and reduce scattering losses and to ensure ease of fabrication.

$$p > d \quad p/\lambda_c < 0.25 \quad 1.2d < p \leq 2d \quad (1)$$

In this paper, we initially employ the techniques of appropriate feeding system, impedance matching and increase of substrate height for the objective of enhancing the antenna bandwidth and miniaturization [16, 17]. Furthermore, grounded shorting posts are used in the air substrate [12], of which the height may be readily adjusted [13], as shown in Fig. 2. We then employ the SIW technique as shown in Fig. 3, which is composed of two microstrip substrates, made of Rogers RT/Duroid 5880, with parameters $\epsilon_r = 2.2$, height $h = 125$ mil and loss tangent $\tan \delta = 0.0009$. In Section 3, the proposed antennas are simulated using an electromagnetic solver, Ansoft HFSS, and the simulation results are shown in good agreement with measurement ones.

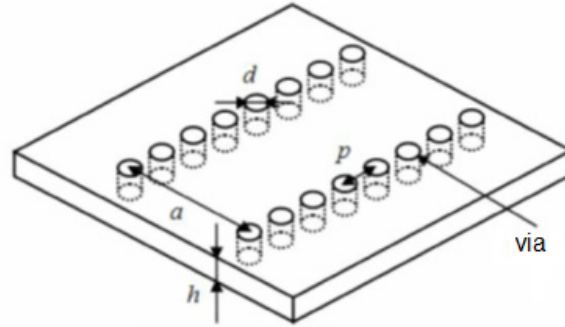


Figure 1. SIW structure.

2. DESCRIPTION OF PROPOSED ANTENNA STRUCTURES

In this paper, we use the antenna probe feeding through a coaxial cable, which has several advantages compared to a microstrip feeding system, such as lower feed line losses, less undesired radiation and adjustability of input impedance by the variation of probe position. In general, a microstrip patch antenna with a probe feeding has a narrow impedance bandwidth due to its high quality factor Q . The increase of substrate height leads to the reduction of Q and increase of its bandwidth. On the other hand, longer probes lead to the increase of their inductive effects which limit the antenna bandwidth.

Several methods have been proposed to overcome such effects, such as folded-patch-feeds [14, 15]. Now, in this paper, we propose an open cavity under patch to decrease the substrate thickness at the probe feed section as shown in Fig. 2(a), whereas the substrate thickness under the patch is kept high. So, the inductive effect of the probe is kept low, and the antenna bandwidth remains high. The operation of UWB in these antennas is obtained using an open cavity above the probe feeding, and the energy coupling to the patch is done through the open cavity. Also, the capacitance of the open cavity cancels the inductive effect of the probe in wide range of frequency. In other words, the presence of open cavity leads to the reduction of effective dielectric constant of structure, so the Q and bandwidth of the antennas will be reduced. Furthermore, the proposed feeding system increases the effective length of patch, while its physical length is kept constant. Consequently, the antenna is effectively miniaturized.

In this article, two types of antenna configurations are designed, fabricated and measured. The first antenna type is shown in Fig. 2, where its detailed geometrical configuration is indicated. Two versions of this configuration are considered, which are called Antenna 1 and Antenna 2. Antenna 1 is designed for the frequency band 2.8 to 11.1 GHz, which is a UWB antenna (Fig. 14). Antenna 2

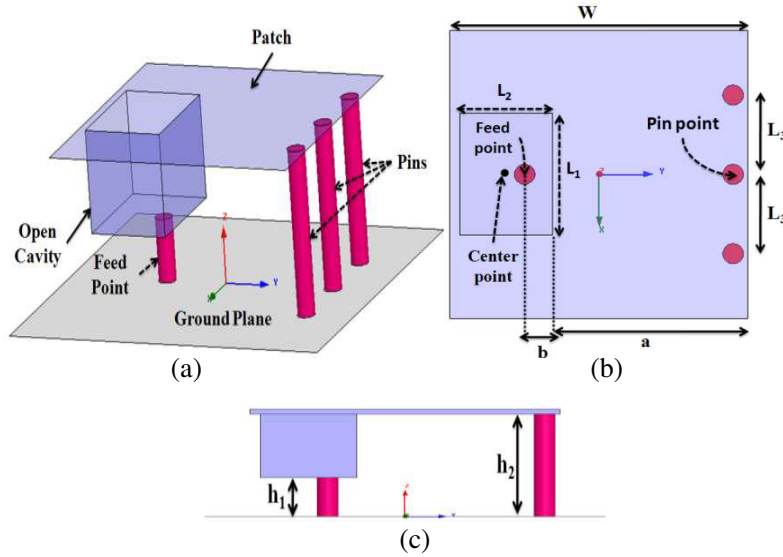


Figure 2. Definition of parameters used in design of the first antenna type.

is fabricated in the frequency band of 0.86 to 3.21 GHz, namely a wireless antenna (Fig. 15). The geometrical dimensions of these two antennas are given in Table 1. The second antenna type is shown in Fig. 3. One version of its configuration is fabricated, which is called Antenna 3 (Fig. 16). The geometrical dimensions of antenna 3 are given in Table 2.

The first antenna type has a smaller size and wider bandwidth relative to other comparable antennas in the literature. The air spacing under the patch has a height of h_2 , whereas the feed probe length (h_1) is shorter. In order to further decrease the antenna size, three shorting pins are installed between the patch and ground plane. The diameters of these pins are optimized to the value of 0.7 mm (see Fig. 2).

The second antenna type applies a substrate integrated resonator (SIR) to the first antenna type, as shown in Fig. 3. It consists of two substrates. Its feed consists of a coaxial probe in the lower substrate connected to a small patch on the interface between the lower and upper substrates. Then this small patch is connected to the upper larger patch on the upper substrate by some pins, in the form of an SIR, which is equivalent to the open cavity in the feeding system of the first antenna type. Also, three shorting pins are connected between the patch and ground plane. Observe that the feed probe is connected to the center of the lower patch. The height of the upper patch to the ground plane is 250 mil, and that of the middle patch is 125 mil. A photograph of the fabricated version of this antenna is shown in Fig. 16. It is observed that its efficiency may be degraded due to the losses in metallic pins.

3. SIMULATION RESULTS AND MEASUREMENT DATA

Firstly, we consider two versions of the first proposed antenna type, denoted as antennas 1 and 2. We then study the second proposed antenna type denoted by antenna 3.

Antenna 1 is designed for the frequency band 2.8 to 11.1 GHz, which is a UWB antenna. The dimensions of antenna 1 are given on Table 1. Its size at the lowest frequency is $0.186\lambda_{f \min} \times 0.186\lambda_{f \min} \times$

Table 1. Dimensions of the first proposed antennas.

	L_1 (mm)	L_2 (mm)	L_3 (mm)	W (mm)	h_1 (mm)	h_2 (mm)	Pin Point (mm)	Feed Point (mm)	Center Point (mm)
Antenna 1	8.4	6.2	5.5	20	4	10.5	(0, 9)	(0, -5)	(0, -6.2)
Antenna 2	32.6	4.6	15	70	5.6	30	(0, 32)	(0, -21.8)	(0, -21.8)

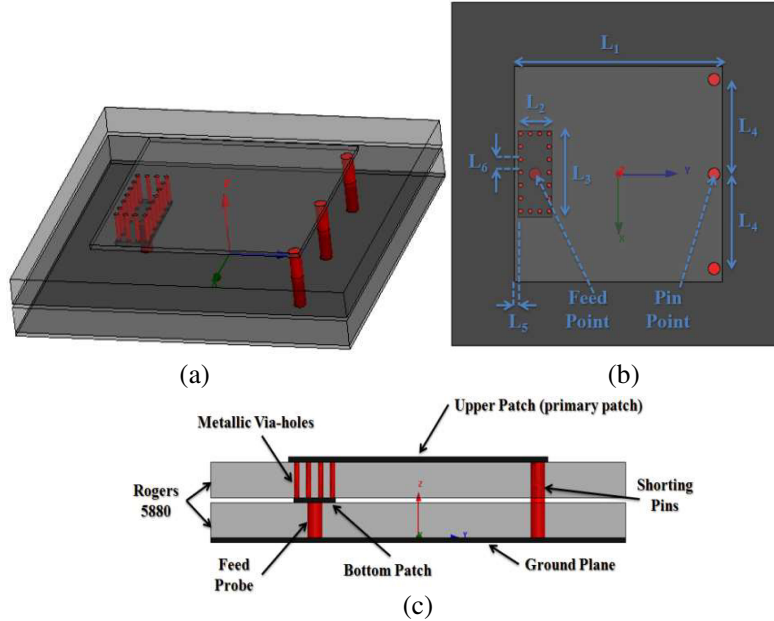


Figure 3. Definition of parameters used in design of the second antenna type.

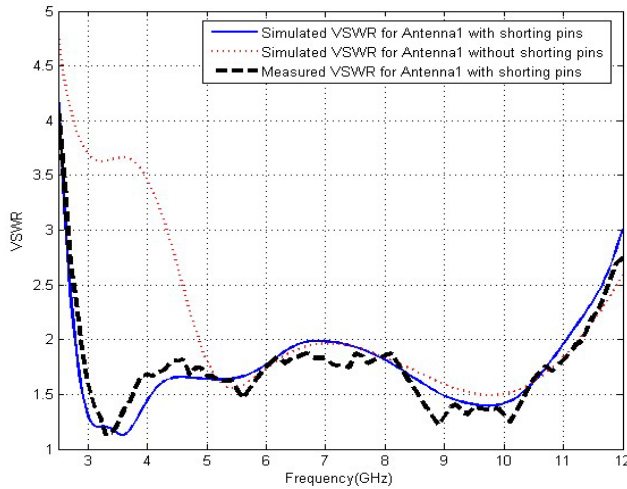


Figure 4. Simulated and measured VSWS of Antenna 1 with and without shorting pins.

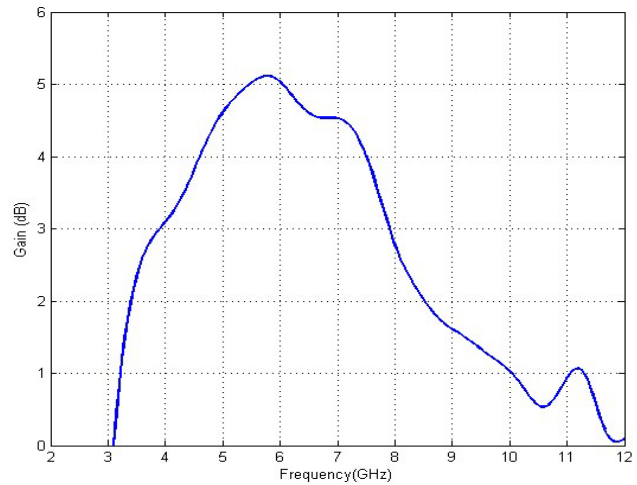


Figure 5. Simulated gain of Antenna 1.

$0.098\lambda_{f_{min}}$. Its impedance bandwidth (for $SWR \leq 2$) is about 119%, which is better than three times of the bandwidth obtained by the common E-shaped patch antenna [10]. Fig. 4 shows the SWR versus frequency for antenna 1 with and without shorting pins as obtained by the simulation results (by HFSS version 12) and measurement data. It is seen that the shorting pins improve VSWR of the antenna for lower frequencies (especially for $f < 5$ GHz). Also, the simulation results are in good agreement with the measurement ones.

To show the degree of miniaturization of the proposed antenna 1, we compare it with the antenna in [9] with size $0.198\lambda_{f_{min}} \times 0.198\lambda_{f_{min}} \times 0.093\lambda_{f_{min}}$ which has obtained a bandwidth of 73.8% in the frequency band 3.96 to 8.59 GHz. It is observed that the bandwidth of antenna 1 has been increased by 45.2% and its size decreased by 11.8%. The gain of antenna 1 is drawn in Fig. 5. The maximum gain is found to be 5.2 dBi while the minimum is 0 dBi. The peak gain is obtained at 5.8 GHz. The delay group is an important parameter of UWB antenna and displays the distortion of the transmitted

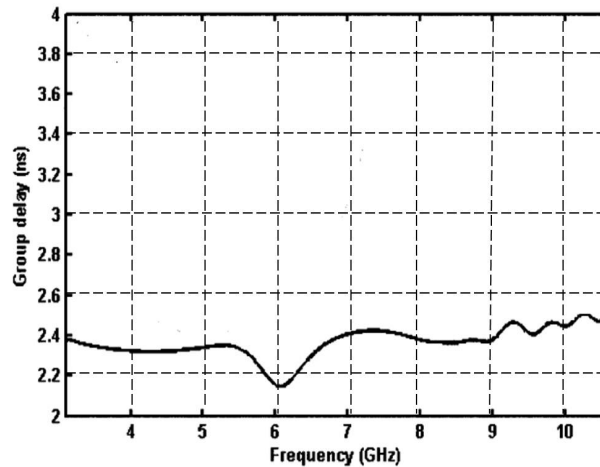


Figure 6. Simulated group delay of Antenna 1.

pulses in the UWB communication. Fig. 6 shows the simulated group delay of antenna 1. It is observed that the group delay is less than 2.5 ns and is almost constant for the entire UWB. So, all frequency components of the UWB pulses propagate in the free space almost with the same delay. The proposed UWB antenna is suitable for UWB communication.

The simulated and measured radiation patterns of antenna 1 in the xz and yz planes are shown in Fig. 7, which is seen to be almost stable across the design bandwidth (especially in xz -plane). It is observed that the radiation patterns display a directional behavior for E_φ with main lobe direction at 0° in the xz -plane. Bi-directional pattern is observed for E_θ in the xz -plane with its main lobe direction at 90° and 270° . It is also obvious that more lobes are observed at the higher frequency. Also, the level of cross-polarization is small compared with the level of co-polarization in yz -plane (H -plane). This pattern is suitable for application in most wireless communication equipment.

The dimensions of the second version of antenna type 1 (namely antenna 2) are given in Table 1. Its SWR is drawn in Fig. 8. Its impedance bandwidth (defined for $SWR \leq 2$) is 115.5% in the frequency band 0.86 to 3.21 GHz. It is observed that the proposed feed system may be applied to any patch size and shape to obtain wide bandwidths. The current distributions on the structure of antenna 1 at the lower and upper limits of the frequency band are shown in Fig. 9. It extends over the whole structure at the lower frequency limit, but it is concentrated at the pin locations at the higher frequency limit.

We then consider the proposed antenna type 2, denoted as antenna 3. Its dimensions are given Table 2. The curves of SWR versus frequency as obtained by computer simulation and measurement for the two cases of with and without substrates are drawn in Fig. 10 (The case of absence of substrate is actually antenna type 1). This antenna can radiate effectively in the band 5.1 to 11.9 GHz for $SWR \leq 2$. Its impedance bandwidth is about 80%. The lower bandwidth of the antenna with no substrate is due to the inappropriate impedance matching, which may be remedied by increasing the height of space under the patch. The impedance matching and bandwidth of antennas for the case of inclusion of substrates may also be improved by increasing the height of substrates. The gain of antenna 3 is drawn in Fig. 11, which has decreased across the band due to the losses of substrate. The advantages of antenna 3 relative to antennas type 1 are the reduction of its size without the increase of its substrate height and its higher bandwidth. Its disadvantage is the reduction of its gain.

Table 2. Dimensions of the antenna 3.

L_1 (mm)	L_2 (mm)	L_3 (mm)	L_4 (mm)	L_5 (mm)	L_6 (mm)	Pin Point (mm)	Feed point (mm)
25	4	10	11	0.5	1	(0, 11.5)	(0, -10)

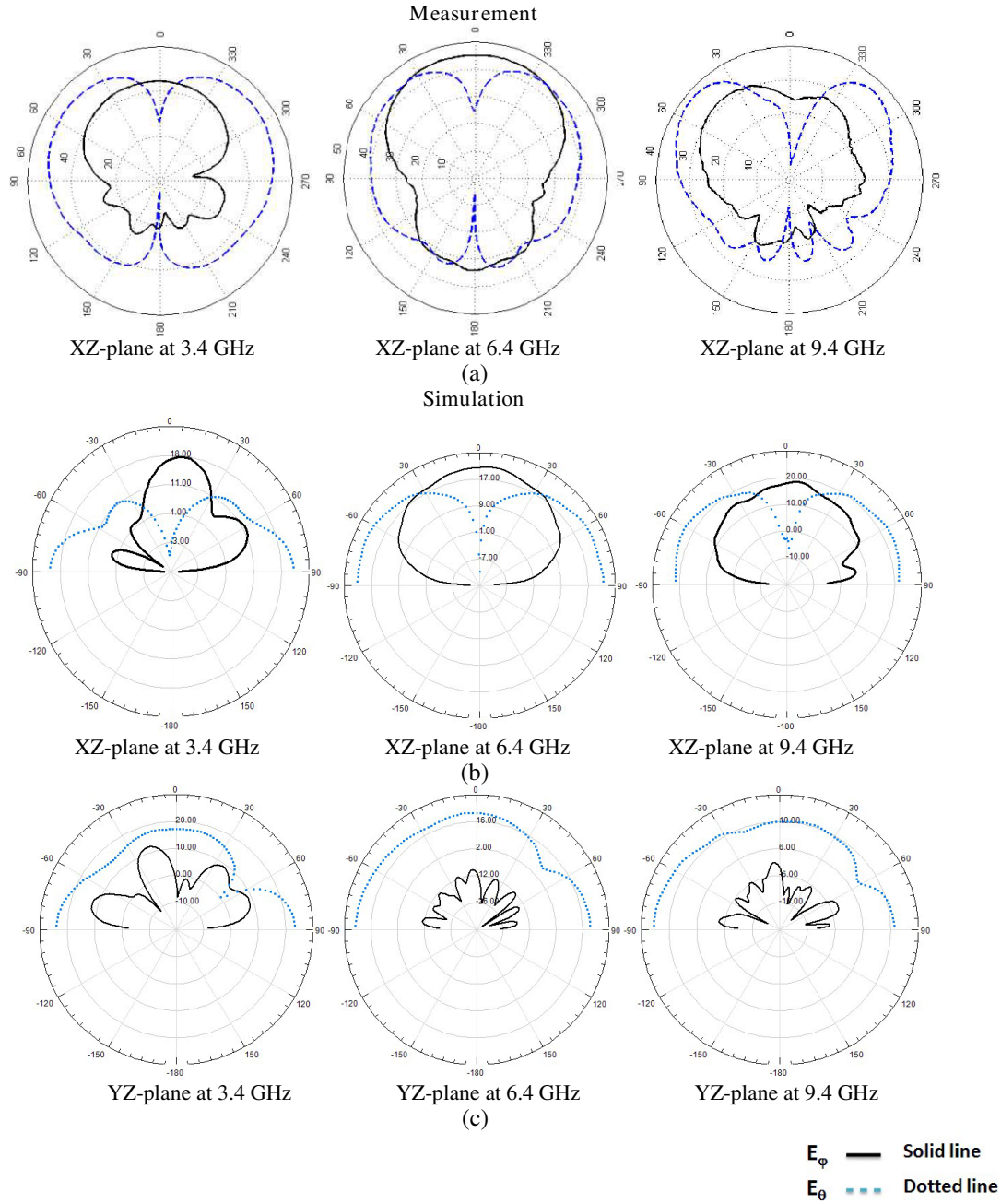


Figure 7. Computer simulated and measured radiation patterns of the antenna 1: (a) measured pattern in the xz -plane ($\varphi = 0^\circ$) (E -plane); (b) simulated pattern in the xz -plane (E -plane); (c) simulated pattern in the yz -plane ($\varphi = 90^\circ$) (H -plane).

The current distributions on the patch of antenna 3 at lower and upper frequencies of the band are drawn in Fig. 12. It is observed that the current distribution at the lower frequency limit extends over the whole structure of antenna and at the upper frequency limit is located at the pins.

The two-dimensional radiation patterns in the xz and yz planes as obtained by simulation and measurements are drawn in Fig. 13 for comparison. The radiation patterns display a directional behavior for E_φ with its main lobe direction at 0° in the xz -plane for three frequencies. Bi-directional pattern for E_θ is observed in the xz -plane with a null at 0° . It is observed that two main lobes of the pattern approach each other with increase of frequency. It is found that the antenna has nearly good

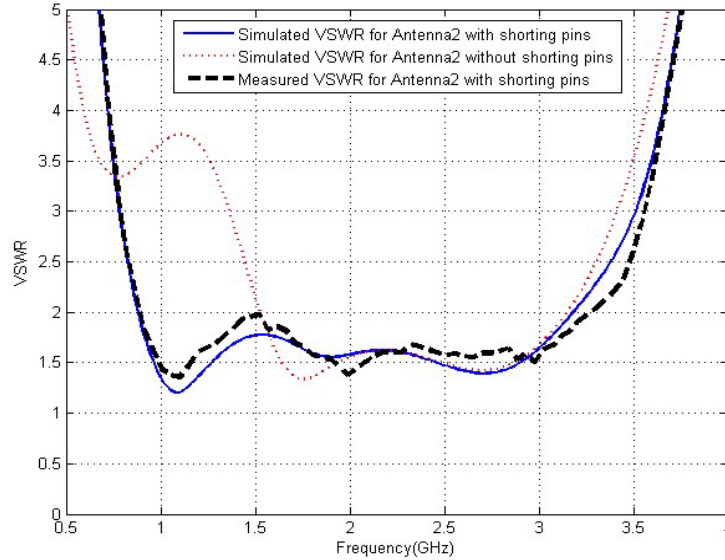


Figure 8. Simulated and measured VSWRs of Antenna 2 with and without shorting pins.

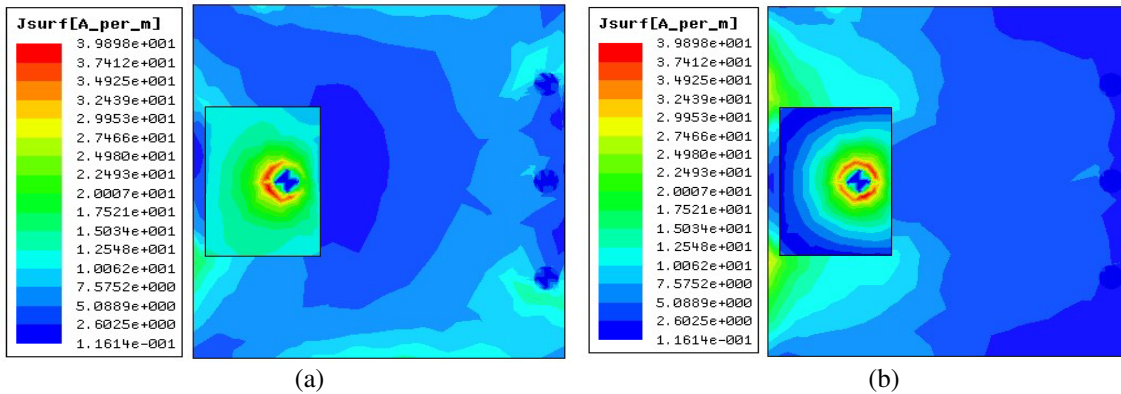


Figure 9. Current distribution on antenna 1 at different frequencies; (a) Current distribution at 2.8 GHz. (b) Current distribution at 11.1 GHz.

omnidirectional radiation patterns at all frequencies in the H -plane. Also, the level of cross-polarization is small compared with the level of co-polarization in the yz -plane (H -plane). It is also observed that simulated results show a good agreement with measured ones.

Table 3 shows the comparison of the antenna characteristics with the recent UWB antennas. It is seen that the level of miniaturization is better than what have been achieved by other comparable techniques reported in the literature.

Table 3. Comparison of the proposed antennas with the previous works.

	Dimensions (mm)	frequency range (GHz)	Bandwidth (%)	Max. Gain (dB)
Antenna 1	$20 \times 20 \times 10.5$	2.8–11.1	119%	5.2
Antenna 3	$25 \times 25 \times 6.35$	5.2–11.5	75.5%	11
Ref. [19]	$28 \times 24 \times 1.6$	3.1–111	112.7%	4.7
Ref. [20]	$25 \times 25 \times 1.6$	2.6–13.04	133.5%	5

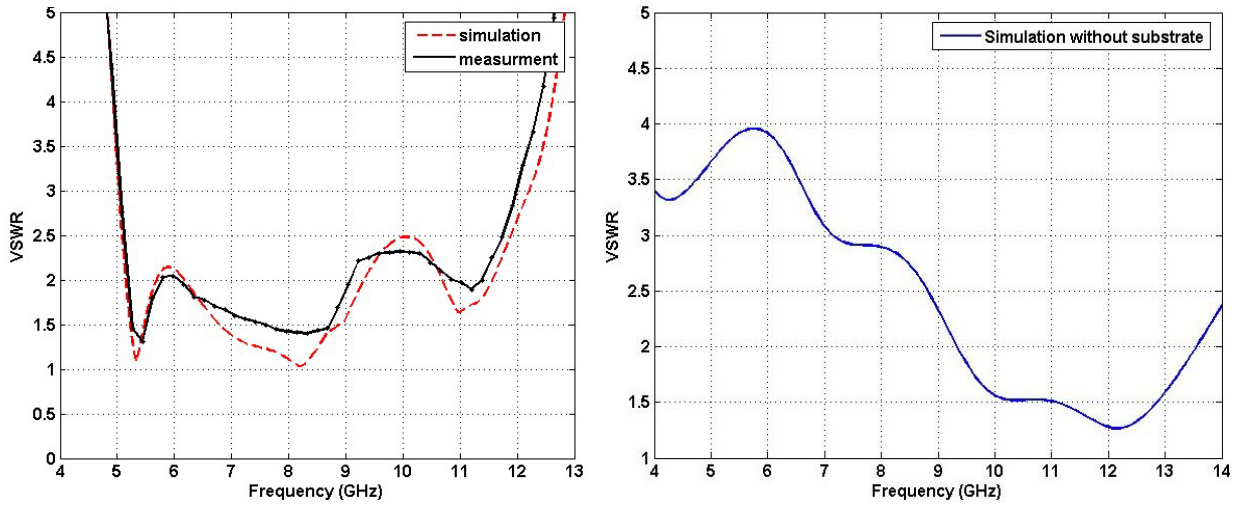


Figure 10. Simulated and measured VSWRs of Antenna 3 with and without substrate.

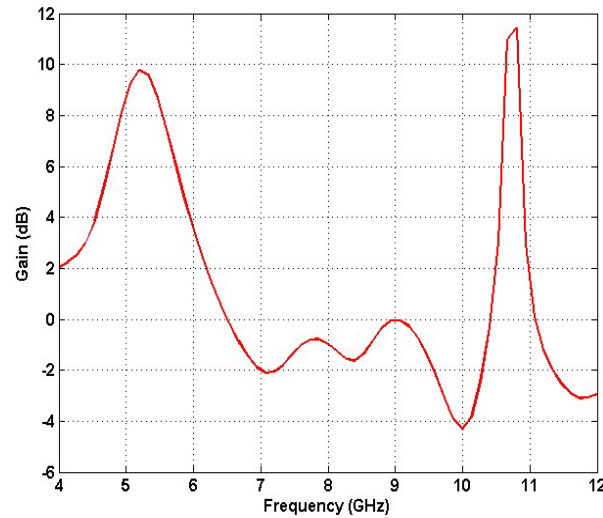


Figure 11. Simulated gain of Antenna 3.

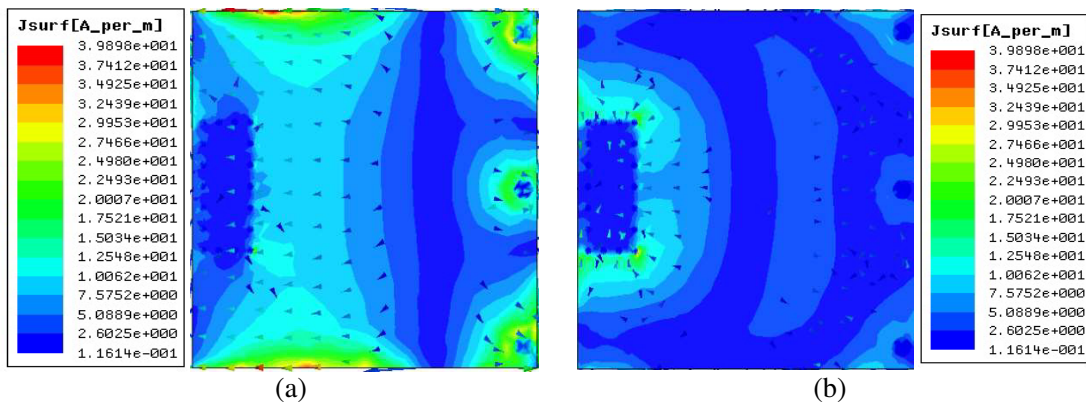


Figure 12. Current distribution on antenna 3 at different frequencies; (a) Current distribution at 5.1 GHz. (b) Current distribution at 11.9 GHz.

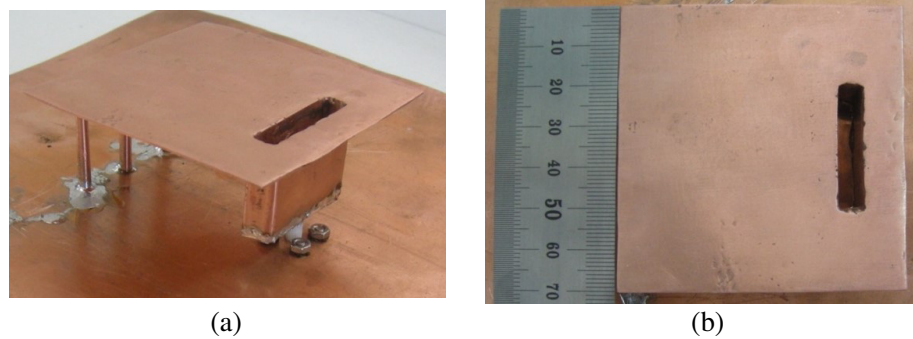


Figure 15. Photograph of antenna 2.

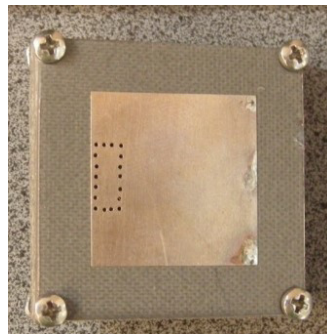


Figure 16. Photograph of antenna 3.

4. CONCLUSION

In this paper, two novel feeding systems are proposed for the miniaturization and realization of wideband performance of microstrip antennas, namely an open cavity resonator (in an air substrate) and a surface integrated resonator (in a dual dielectric substrate), both fed by a coaxial probe. Three prototype models are fabricated and measured, namely two patch antennas with three shorting pins with an air cavity, one for operation in UWB (3.1–10.6 GHz) and the other for GPS (1.5–1.8 GHz), WiFi (2.1–2.6 GHz) and Wireless (3.1–3.8 GHz). A third patch antenna with an SIW cavity is fabricated for UWB. The level of miniaturization and ultra-wideband performance are better than what have been achieved by other comparable techniques reported in the literature.

REFERENCES

1. Skrivervik, A. K., J.-F. Zurcher, O. Staub, and J. R. Mosig, "PCS antenna design: The challenge of miniaturization," *IEEE Antennas and Propagation Magazine*, Vol. 43, 12–27, Aug. 2001.
2. Wei, L.-A., "Applications of ultra wideband," M.S., The University of Texas at Arlington, Dec. 2006.
3. Kula, J. S., D. Psychoudakis, W.-J. Liao, C.-C. Chen, J. L. Volakis, and J. W. Halloran, "Patch-antenna miniaturization using recently available ceramic substrates," *IEEE Antennas and Propagation Mag.*, Vol. 48, No. 6, Dec. 2006.
4. Chen, D. and C.-H. Cheng, "A novel compact ultra-wideband (UWB) wide slot antenna with via holes," *Progress In Electromagnetic Research*, Vol. 94, 343–349, 2009.
5. Schaubert, D. H., D. M. Pozar, and A. Adrian, "Effect of microstrip antenna substrate thickness and permittivity: Comparison of theories and experiment," *IEEE Trans. Antennas Propag.*, Vol. 37, 677–682, Jun. 1989.

6. Poes, H. F. and A. R. Van De Capelle, "An impedance-matching technique for increasing the bandwidth of microstrip antennas," *IEEE Trans. Antennas Propag.*, Vol. 37, No. 11, 1345–1354, Nov. 1989.
7. Kumar, G. and K. C. Gupta, "Broad-band microstrip antennas using additional resonators gap-coupled to the radiating edges," *IEEE Trans. Antennas Propag.*, Vol. 32, 1375–1379, Dec. 1984.
8. Wi, S.-H., J.-M. Kim, T.-H. Yoo, H.-J. Lee, J.-Y. Park, J.-G. Yook, and H.-K. Park, "Bow-tie-shaped meander slot antenna for 5 GHz application," *Proc. IEEE Int. Symp. Antenna and Propagation*, Vol. 2, 456–459, Jun. 2002.
9. Li, Y., W. Hong, G. Hua, J. Chen, K. Wu, and T. J. Cui, "Simulation and experiment on SIW slot array antennas," *IEEE Microwave Wireless Compon. Lett.*, Vol. 14, No. 9, 137–139, Sep. 2004.
10. Hong, W., B. Liu, G. Q. Luo, Q. H. Lai, J. F. Xu, Z. C. Hao, F. F. He, and X. X. Yin, "Integrated microwave and millimeter wave antennas based on SIW and HMSIW technology," *IEEE Microw. Antennas and Propagation*, 69–72, 2007.
11. Zhang, X.-C., Z.-Y. Yu, and J. Xu, "Novel band-pass substrate integrated waveguide (SIW) filter based on complementary split ring resonators (CSRRS)," *Progress In Electromagnetics Research*, Vol. 72, 39–46, 2007.
12. Sotoodeh, Z., B. Biglarbegan, and F. H. Kashani, "A novel bandpass waveguide filter structure on SIW technology," *Progress In Electromagnetics Research Letters*, Vol. 2, 141–148, 2008.
13. Xu, H., J. Lei, C. Cui, and L. Yang, "UWB dual-polarized Vivaldi antenna with high gain," *2012 International Conference on Microwave and Millimeter Wave Technology (ICMMT)*, Vol. 3, 1, 4, 5–8, May 2012.
14. Chiu, C. Y., H. Wong, and C. H. Chan, "Study of small wideband folded-patch-feed antennas," *IET Microw. Antennas and Propagation*, Vol. 1, No. 2, 501–505, 2007.
15. Naser-Moghadasi, M., A. Dadgarpour, F. Jolani, and B. S. Virdee, "Ultra wideband patch antenna with a novel folded-patch technique," *IET Microw. Antennas and Propagation*, Vol. 3, No. 1, 164–170, 2009.
16. Oraizi, H. and S. Hedayati, "Miniaturized UWB monopole microstrip antenna design by the combination of Giuseppe Peano and Sierpinski carpet fractals," *IEEE Antennas and Wireless Propagation Letters*, Vol. 10, No. 1, 67–70, Jan. 28, 2011.
17. Madhav, B. T. P., V. G. K. M. Pisipati, H. Khan, and P. V. Datta Prasad, "Shorting plate planar inverted folded antenna on LC substrate for bluetooth applications," *Journal of Engineering Science and Technology Review*, 42–45, Aug. 2012.
18. Guha, D. and Y. M. M. Antar, *Microstrip and Printed Antennas*, Ch. 10, John Wiley & Sons Ltd., 2011.
19. Abbas, S. M., Y. Ranga, A. K. Verma, and K. P. Esselle, "A simple ultra wideband printed monopole antenna with high band rejection and wide radiation patterns," *IEEE Trans. Antennas Propag.*, Vol. 62, No. 9, 4816–4820, Sept. 2014.
20. Gautam, A. K., S. Yadav, and B. K. Kanaujia, "A CPW-fed compact UWB microstrip antenna," *IEEE Antennas and Wireless Propagation Letters*, Vol. 12, 151–154, Jan. 2013.